Weak measurement with the peak-contrast-ratio pointer

Junfan Zhu, Zhaoxue Li, Yurong Liu, Yucheng Ye, Qian Ti, Zhiyou Zhang,* and Fuhua Gao†
College of Physics, Sichuan University, Chengdu 610064, China

(Received 7 December 2020; accepted 2 March 2021; published 16 March 2021)

Weak measurement as a nonperturbative theory has been shown to be powerful in the fundamentals of quantum mechanics and high-precision metrology, in which the pointer is of great importance to parameter estimation and experimental design. In this work, we find that under the conditions of weak coupling and Gaussian meter, the probability distribution after the postselection follows a bimodal function and the peak contrast ratio (PCR) can be applied as a special pointer, which is different from the shift of mean value. To obtain the PCR, only two values corresponding to the two peaks in the distribution function are required. We theoretically present the relation of the PCR and parameters to be estimated, and then demonstrate it in an experiment. Weak measurement with the PCR pointer has the advantages of reducing the requirements of the apparatus and suppressing noise, which also provides a heuristic approach for studying weak measurement when the weak value is very large.

DOI: 10.1103/PhysRevA.103.032212

I. INTRODUCTION

Since the evolution of a quantum system is driven both by the Hamiltonian and measurements, compared with classical measurements, quantum measurements are much more intriguing. For an understanding of the role of measurements in quantum mechanics, von Neumann developed a standard model to describe how the quantum system and the measurement meter are coupled [1]. The concept of the pre- and postselected measurement was originally proposed by Aharonov *et al.* to study the time symmetry problem in the quantum process [2]. When the coupling strength between the system and the meter is sufficiently small, the pre- and postselected measurement is in a weak measurement scheme. Aharonov *et al.* theoretically found that the result of a measurement of a component of the spin-$1/2$ particle can be amplified by a large number called "the weak value" [3], which opened up a gate for the study of weak measurement in various fields.

For now, the widely used pointer in weak measurement is the shift of mean value (SMV), such as the coordinate shifts [4–8], the momentum shifts [9–11], the frequency shifts [12–19], the temporal shifts [20,21], the angular rotation shifts [22], and the photon number shifts [23,24]. According to the mathematical expression of the SMV, its working region can be divided into three parts, which are named the linear response region, the intermediate region, and the inverted region, respectively [25]. Nevertheless, most of the previous studies were confined to the linear response region. In the linear response region, the SMV can be amplified linearly by the weak value, which is known as the weak value amplification technique. However, since the weak value is restricted by the uncertainty of the meter wave function, the SMV may still be imperceptible if the uncertainty is tiny. So, in order to extend the application of weak measurement, new approaches which can allow the weak value to be large are demanded. Another problem often questioned in weak measurement is that when the pre- and postselections are nearly orthogonal, the probability of a successful measurement will be very small [26,27]. To obtain a complete distribution function, the repeated measurement times should be large and the requirements of the detecting apparatus are strict. For example, the resolution of the apparatus should be high enough and the detecting range should be broad. Furthermore, it has been found that although certain types of technical noise can be suppressed in weak measurement [28–30], the disturbance to the distribution function cannot be underestimated, which inevitably increases the difficulty of obtaining an accurate SMV. Many efforts have been made to solve these problems. For instance, the power-recycled metrology was proposed to eliminate the inefficiency of the rare probability [31]. Some research also used a split-detection method to reduce the requirement of the apparatus resolution [32–34]. However, in these efforts, the complete distribution function is still necessary.

Here we propose another pointer, the peak contrast ratio (PCR). Under the conditions of weak coupling and Gaussian meter, we theoretically show that two values corresponding to the two peaks in the distribution function are already enough for realizing weak measurement. With the PCR pointer, the weak value can be very large and obtaining a complete distribution function is not necessary indeed. We also show that the noise can be suppressed well. Finally, a proof-of-principle experiment is presented to confirm the availability of the PCR pointer.

This paper is organized as follows. In Sec. II, we start with the theory of weak measurement and present the distribution functions after the postselection in x and p spaces. In Sec. III, we introduce the PCR pointer to realize weak measurement. In Sec. IV, we describe the experimental setup and discuss the

*zhangzhiyou@scu.edu.cn
†gaofuhua@scu.edu.cn

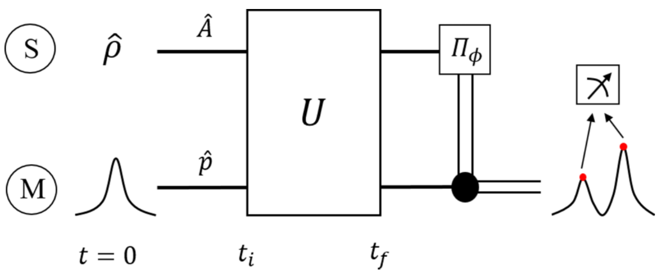

FIG. 1. Schematic diagram of weak measurement with the PCR pointer. S denotes the system and M denotes the meter. The single and double lines correspond to the quantum and classical processes, respectively.

results. Finally, a brief conclusion is drawn in Sec. V. For the sake of simplicity, we make $\hbar = 1$ and often omit inessential factors by using the proportionality sign "$\propto$" instead of the exact equality sign "=".

II. WEAK MEASUREMENT SCHEME

As shown in Fig. 1, let us consider a pre- and postselected measurement scheme in which a system ρ and a meter ρ_m are in the pure states $|\psi\rangle$ and $|\psi_m\rangle$, respectively. The coupling is turned on in the time interval (t_i, t_f). Then, a projective measurement $\Pi_\phi = |\phi\rangle\langle\phi|$, to the system only, play a role of the postselection. Finally, a pre- and postselected measurement is accomplished after reading out the pointer corresponding to the variable x or p of the meter, where x and p satisfy the commutation relation $[\hat{x}, \hat{p}] = i$. It should be noted that here x and p do not represent coordinate and momentum particularly.

According to the von Neumann measurement model, the system and the meter are coupled by the interaction described by the Hamiltonian [1,3]

$$H = g(t)\hat{A} \otimes \hat{p}, \tag{1}$$

with $g(t)$ the instantaneous coupling rate, $\hat{A}$ the operator corresponding to the measured quantity A of the system, and $\hat{p}$ the operator corresponding to p. Hence by solving the Schrödinger equation, the unitary transformation U can be obtained, which takes the form

$$U = \exp\left(-i\int_{t_i}^{t_f} H dt\right) = \exp(-i\gamma\hat{A} \otimes \hat{p}), \tag{2}$$

where $\gamma = \int_{t_i}^{t_f} g(t)dt$ is defined as the coupling strength.

Following the previous approach, we take the meter wave function as a Gaussian, which in x or p space is presented as

$$\psi_m(x) \propto \exp\left[-\frac{(x-\overline{x})^2}{4(\Delta x)^2}\right] \tag{3}$$

or

$$\psi_m(p) \propto \exp\left[-\frac{(p-\overline{p})^2}{4(\Delta p)^2}\right], \tag{4}$$

where $\overline{x}$, $\overline{p}$ and Δx, Δp are, respectively, the mean values and the uncertainties of x and p at $t = 0$.

The word "weak" of weak measurement is usually understood in a way that the coupling strength in a pre- and postselected measurement is sufficiently small. In order to figure out how small of a coupling strength can be considered sufficient, we can express the Hermitian operator $\hat{A}$ with eigenvalues a_i and a complete set of orthonormal eigenvectors $|a_i\rangle$ as $\hat{A} = \sum_i a_i|a_i\rangle\langle a_i|$ and the pure states $|\psi\rangle$ of the system as $|\psi\rangle = \sum_i c_i|a_i\rangle$, with $|c_i|^2$ indicating the probability of finding the system in eigenstate $|a_i\rangle$. In a standard measurement, which refers to a measurement without the postselection, the coupled state of the system and the meter in x space is given by

$$\begin{aligned}|\psi_f(x)\rangle &= \langle x|\exp(-i\gamma\hat{A}\otimes\hat{p})|\psi\rangle|\psi_m\rangle \\ &= \langle x|\sum_i \exp(-i\gamma a_i\hat{p})c_i|a_i\rangle|\psi_m\rangle \\ &= \sum_i c_i\psi_m(x-\gamma a_i)|a_i\rangle.\end{aligned} \tag{5}$$

A projective measurement performing on eigenstate $|a_i\rangle$ will lead to a corresponding wave packet $\psi_m(x-\gamma a_i)$. However, when the distance between any two wave packets $\psi_m(x-\gamma a_i)$ and $\psi_m(x-\gamma a_j)$ is much smaller than the uncertainty of x, which may be represented as

$$|\gamma(a_i - a_j)| \ll \Delta x, \tag{6}$$

the two wave packets will severely overlap so that a measurement will provide almost no information. In our case where the wave function $\psi_m(x)$ follows a Gaussian, there is a saturated uncertainty relation $\Delta x\Delta p = 1/2$ [35]. Then, Eq. (6) can be further rewritten as

$$|\gamma(a_i - a_j)|\Delta p \ll 1. \tag{7}$$

As long as the coupling strength is so weak that Eq. (6) or (7) is generally satisfied, we should deem that the pre- and postselected measurement is in a weak measurement scheme. In weak measurement, the unitary transformation can be expanded and held up to the first-order term only, namely (see Appendix A),

$$U = \exp(-i\gamma\hat{A}\otimes\hat{p}) \simeq 1 - i\gamma\hat{A}\otimes\hat{p}. \tag{8}$$

Under this circumstance, the distribution functions after the postselection in the x and p spaces will take the following forms, respectively (see Appendix B):

$$\begin{aligned}\Phi(x) &= \mathrm{Tr}[(|x\rangle\langle x|\otimes\Pi_\phi)U(\rho\otimes\rho_m)U^\dagger] \\ &\propto \left\{1 + \frac{\gamma(x-\overline{x})}{(\Delta x)^2}\mathrm{Re}A_w + \left[\frac{\gamma(x-\overline{x})}{2(\Delta x)^2}\right]^2|A_w|^2\right\} \\ &\quad\times|\langle\phi|\psi\rangle|^2\exp\left[-\frac{(x-\overline{x})^2}{2(\Delta x)^2}\right]\end{aligned} \tag{9}$$

and

$$\begin{aligned}\Phi(p) &= \mathrm{Tr}[(|p\rangle\langle p|\otimes\Pi_\phi)U(\rho\otimes\rho_m)U^\dagger] \\ &\propto \{1 + 2\gamma p\mathrm{Im}A_w + \gamma^2p^2|A_w|^2\} \\ &\quad\times|\langle\phi|\psi\rangle|^2\exp\left[-\frac{(p-\overline{p})^2}{2(\Delta p)^2}\right],\end{aligned} \tag{10}$$

where $A_w = \langle\phi|\hat{A}|\psi\rangle/\langle\phi|\psi\rangle$ is the so-called weak value. The weak value has many novel properties [26,36–40]. For example, it is generally arbitrary in the complex space.

III. THE PEAK-CONTRAST-RATIO POINTER

In the previous studies of weak measurement, with the distribution functions presented above, the usually used pointer is the SMV, which is given by

$$\delta\langle x\rangle = \frac{\int_{-\infty}^{+\infty}(x-\overline{x})\Phi(x)dx}{\int_{-\infty}^{+\infty}\Phi(x)dx}$$
$$\text{or}\quad \delta\langle p\rangle = \frac{\int_{-\infty}^{+\infty}(p-\overline{p})\Phi(p)dp}{\int_{-\infty}^{+\infty}\Phi(p)dp}. \tag{11}$$

In order to obtain the SMV, we need to detect the complete distribution function, which may be not practically easy. When the pre- and postselections are nearly orthogonal, which means $|\langle\phi|\psi\rangle|^2 \ll 1$, the probability after the postselection will be quite small. Thus the repeated measurement times should be large enough. On the other hand, the detecting range of the apparatus should be broad. The resolution in x or p space should be high enough as well to follow the Nyquist sampling theorem [41]. However, the improvements of the detecting range are usually at the cost of the reductions of resolution, and vice versa. In fact, it can be noted that the distribution function will gradually peak at two points with the measurement times increasing. If we concentrate on the two peaks only and even disregard where they exactly located in x or p space, then obtaining a complete distribution function will be unnecessary. Correspondingly, the repeated measurement times and the requirements for the apparatus can both be reduced. Henceforth, we will show that another pointer, the PCR, may offer a different way to realize weak measurement well.

For the case of the distribution function in x space, we assume that the weak value is purely real for simplicity and then define

$$u = \frac{2(\Delta x)^2}{\gamma A_w}, \tag{12}$$

so that Eq. (9) further becomes

$$\Phi(x) \propto \left[\frac{\gamma(x-\overline{x})}{2(\Delta x)^2}A_w + 1\right]^2 |\langle\phi|\psi\rangle|^2 \exp\left[-\frac{(x-\overline{x})^2}{2(\Delta x)^2}\right]$$
$$\propto [(x-\overline{x})+u]^2 \exp\left[-\frac{(x-\overline{x})^2}{2(\Delta x)^2}\right]. \tag{13}$$

Here what we are concerned about is the u, indicating that the quantity to be measured can be the coupling strength, the weak value, or even the uncertainty of x, as long as the other two parameters are determined. Without much difficulty, we can find that there exist two local maximum points denoted as x_1 and x_3, and one local minimum point denoted as x_2, in the distribution function. The exact expressions of these three points are

$$x_1 = \tfrac{1}{2}[-u-\sqrt{u^2+8(\Delta x)^2}]+\overline{x},$$
$$x_2 = -u+\overline{x}, \tag{14}$$
$$x_3 = \tfrac{1}{2}[-u+\sqrt{u^2+8(\Delta x)^2}]+\overline{x},$$

respectively. So the graph of $\Phi(x)$ consists of two peaks and a valley, and then we can say that $\Phi(x)$ follows a bimodal distribution. When $u=0$, which means that the weak value $A_w \to \infty$, it can be found that $\Phi(x)$ is symmetric about the axis $x=\overline{x}$. However, once u is not equal to zero, $\Phi(x)$ will no longer be symmetric. So we may deem that u plays a role of breaking the symmetry of the distribution function. In addition, when A_w is not so large that the condition $|\gamma A_w| \ll \Delta x$ is satisfied, it can be found that $x_3 \simeq |\gamma A_w| + \overline{x}$, which presents the well-known linear relation between the SMV and the coupling strength.

Now given the two maximum points x_1 and x_3, the PCR can be obtained, which is defined by

$$R_x = \frac{\Phi(x_3)-\Phi(x_1)}{[\Phi(x_3)+\Phi(x_1)]/2}$$
$$= \frac{2(\alpha_+e^{-\alpha_-}-\alpha_-e^{-\alpha_+})}{\alpha_-e^{-\alpha_+}+\alpha_+e^{-\alpha_-}}, \tag{15}$$

where $\alpha_\pm = [u\pm\sqrt{u^2+8(\Delta x)^2}]^2/8(\Delta x)^2$. It is easy to find that R_x is in an odd function of u, an intuitive understanding of which is that the positions of the left and right peaks are exchanged as the sign of u changes. For the case that $|u| \ll \Delta x$, Eq. (15) can be simplified to

$$R_x \simeq 2\sqrt{2}(\Delta x)^{-1}u, \tag{16}$$

which indicates a linear relation between R_x and u. Thus we may call the region where $|u| \ll \Delta x$ as the linear response region. We should note that since the PCR is taken as the pointer, the linear response region defined here is quite different from the traditional linear response region when the SMV is taken as the pointer. Taking into account the exact expression of u, the linear response region of the PCR can be further written as $\Delta x \ll |\gamma A_w|$. However, as mentioned above, the linear response region of the SMV reads $|\gamma A_w| \ll \Delta x$. Therefore, the PCR pointer provides a heuristic approach for studying weak measurement when the weak value is very large. If we intend to measure γ or A_w, we are encouraged to reduce the value of Δx to increase the corresponding dynamical range. On the other hand, if we intend to measure Δx, we can enlarge the values of γ and A_w instead. For the other extreme case that $|u| \gg \Delta x$, it follows that

$$R_x \simeq \pm 2, \tag{17}$$

the correct sign of which depends on the sign of u. Since R_x is constant, we may call the region where $|u| \gg \Delta x$ as the constant region. On account of the independence of R_x and u in the constant region, R_x will provide almost no information of u. So, in practical application of the PCR pointer, we should keep away from the constant region. From Eq. (17), we can also note that the value of R_x ranges from -2 to 2. It is worth emphasizing that the principal condition of weak measurement, i.e., Eq. (6) or (7), must always be satisfied.

For the case of the distribution function in p space, we assume that the weak value is purely imaginary for simplicity and then define

$$v = \frac{1}{\gamma A_w} + \overline{p}. \tag{18}$$

Thus, Eq. (10) can be rewritten as

$$\begin{aligned}\Phi(p) &\propto (\gamma p A_w + 1)^2 |\langle\phi|\psi\rangle|^2 \exp\left[-\frac{(p-\overline{p})^2}{2(\Delta p)^2}\right] \\ &\propto [\gamma A_w(p-\overline{p}) + \gamma A_w \overline{p} + 1]^2 \exp\left[-\frac{(p-\overline{p})^2}{2(\Delta p)^2}\right] \\ &\propto [(p-\overline{p}) + v]^2 \exp\left[-\frac{(p-\overline{p})^2}{2(\Delta p)^2}\right].\end{aligned} \tag{19}$$

It can be noted that Eqs. (13) and (19) take the same form mathematically, so all the discussion above for the distribution function in x space can have its counterpart for the distribution function in p space. Similarly, there exist two local maximum points denoted as p_1 and p_3, and one local minimum point denoted as p_2, which take the following forms, respectively:

$$\begin{aligned}p_1 &= \tfrac{1}{2}[-v - \sqrt{v^2 + 8(\Delta p)^2}] + \overline{p}, \\ p_2 &= -v + \overline{p}, \\ p_3 &= \tfrac{1}{2}[-v + \sqrt{v^2 + 8(\Delta p)^2}] + \overline{p}.\end{aligned} \tag{20}$$

Here, it is the v that plays a role of breaking the symmetry of the distribution function. The PCR in p space now is given by

$$\begin{aligned}R_p &= \frac{\Phi(p_3) - \Phi(p_1)}{[\Phi(p_3) + \Phi(p_1)]/2} \\ &= \frac{2(\beta_+ e^{-\beta_-} - \beta_- e^{-\beta_+})}{\beta_- e^{-\beta_+} + \beta_+ e^{-\beta_-}},\end{aligned} \tag{21}$$

with $\beta_\pm = [v \pm \sqrt{v^2 + 8(\Delta p)^2}]^2 / 8(\Delta p)^2$. Also, R_p is in an odd function of v. In the extreme case that $|v| \ll \Delta p$, we can obtain R_p in the linear response region, which is given by

$$R_p \simeq 2\sqrt{2}(\Delta p)^{-1} v. \tag{22}$$

Taking Eq. (18) into account, the linear response region may be further written as $|\gamma A_w|(\overline{p} + \Delta p) \gg 1$. Hence it can be seen that in order to increase the dynamical range of γ, A_w, or Δp, we should make the other two parameters as large as possible. In the constant region, which should be kept away from, R_p takes the following form:

$$R_p \simeq \pm 2, \tag{23}$$

the correct sign of which depends on the sign of v.

In practical applications, a consideration of the noise which can disturb the distribution function after the postselection is inevitable. Taking the x-space distribution function for an example, we let $\epsilon(x)$ denote the noise function and take the following form:

$$\epsilon(x) = a + b\Phi(x), \tag{24}$$

where a indicates the homogeneous noise and $b\Phi(x)$ indicates the noise which is proportional to the intensity of the distribution function. Both a and b are time dependent. It should be noted that here we do not specifically discuss the types of noise, so that $\epsilon(x)$ can be regarded as the general result of various noises. We may consider that the intensity of the noise is always much smaller than the maximum intensity of the distribution function, namely,

$$\epsilon(x) \ll \max[\Phi(x_1), \Phi(x_3)], \tag{25}$$

which also implies that $a \ll \max[\Phi(x_1), \Phi(x_3)]$ and $b \ll 1$. Then, when the noise is taken into account, the PCR in x space becomes

$$\begin{aligned}R_x^\epsilon &= \frac{\Phi(x_3) + \epsilon(x_3) - \Phi(x_1) - \epsilon(x_1)}{[\Phi(x_3) + \epsilon(x_3) + \Phi(x_1) + \epsilon(x_1)]/2} \\ &\simeq R_x(1+b)\left[1 - b - \frac{2a}{\Phi(x_3) + \Phi(x_1)}\right] \\ &\simeq R_x\left[1 - \frac{2a}{\Phi(x_3) + \Phi(x_1)}\right],\end{aligned} \tag{26}$$

where all the higher-order terms are neglected. On the other hand, when the noise is introduced, the SMV in x space takes the following form (see Appendix C):

$$\delta\langle x\rangle^\epsilon \simeq \delta\langle x\rangle\left[1 - \frac{a}{\Phi(x_0)}\right]. \tag{27}$$

It can be noted that for both the PCR and SMV pointers, it is the homogeneous noise that plays a dominating part. Since $\Phi(x_0)$ is at the same order as $\max[\Phi(x_1), \Phi(x_3)]$, there should be a relation $a \ll \Phi(x_0)$ due to the condition given by Eq. (25). Therefore, it turns out approximately that $R_x^\epsilon \approx R_x$ and $\delta\langle x\rangle^\epsilon \approx \delta\langle x\rangle$, which indicates that the noise can be suppressed well for both of the two pointers. Furthermore, we can obtain that

$$\frac{3}{\sqrt{2\pi}} \leqslant \frac{\Phi(x_3) + \Phi(x_1)}{2\Phi(x_0)} \leqslant \frac{12}{\sqrt{2\pi}e},$$

which also holds for the distribution function in p space. So the PCR pointer is better at suppressing noise, although this effect may not be very significant.

IV. EXPERIMENT

In the following, we propose an experimental protocol, depicted in Fig. 2, to demonstrate the availability of the PCR pointer. A white laser and a following Gaussian filter together constitute the meter state. So the input meter variable is the angular frequency denoted as ω. Since the source used is classical, repeated measurement times just correspond to the light intensity. Then the light beam travels through the first polarizer (P1) which preselects the system at the state

$$|\psi\rangle = \frac{1}{\sqrt{2}}(|H\rangle + |V\rangle), \tag{28}$$

where $|H\rangle$ and $|V\rangle$ represent the horizontal and vertical polarization states, respectively. A half-half wave-plate combination introduces a time delay τ ($\tau = 1.22 \times 10^{-16}$ s), which corresponds to the coupling strength, between the horizontal and vertical polarization states [15]. Thus the operator representing the measured quantity here is

$$\hat{A} = |H\rangle\langle H| - |V\rangle\langle V|. \tag{29}$$

Afterwards, a quarter wave plate (QWP) together with the second polarizer (P2) postselect the system at the state (see

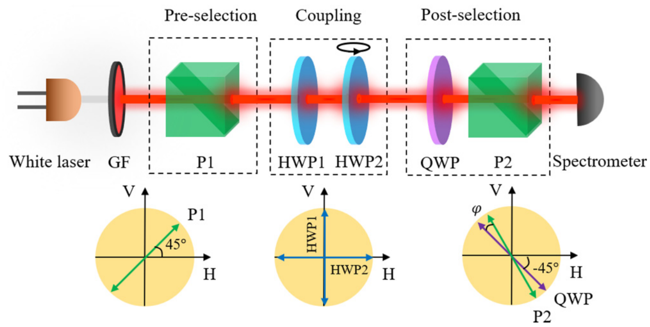

FIG. 2. Experimental setup. A white laser as the light source; GF: Gaussian filter with the central wavelength 633 nm and the FWHM (full width at half maximum) 10 nm; P1 and P2: Polarizers with optical axes set at 45° and $\varphi - 45°$, respectively; HWP1 and HWP2: Half-half wave-plate combination with optical axes perpendicular to each other, the latter one of which can be rotated around its vertical axis by a certain angle to introduce a time delay; QWP: Quarter wave plate with the optical axis set at $-45°$. A spectrometer is used as the detector.

Appendix D)

$$|\phi\rangle \simeq \frac{1}{\sqrt{2}}[\exp(-i\varphi)|H\rangle - \exp(i\varphi)|V\rangle], \tag{30}$$

with φ the angle at which the polarization direction of P2 deviates from $-\pi/4$. Therefore, the weak value can be obtained immediately that

$$A_w = -i\cot\varphi. \tag{31}$$

Since the detecting apparatus is a spectrometer, the input and output meter variables are identical. So it is the PCR defined in Eq. (21) that should be adopted to do weak measurement.

For the purpose of measuring a practically significant quantity, we choose the phase difference, which is defined by

$$\xi = \tau v = -\tan\varphi + \tau\varpi. \tag{32}$$

We first adjust the polarization direction of P2 to make the spectrum after the postselection present the bimodal distribution and then make the intensities of the two peaks exactly the same. In this way, we can figure out that ξ is equal to zero. Under such initial conditions, we next fine tune the polarization direction of P2 so that the value of ξ takes 3.49×10^{-4}, 6.98×10^{-4}, 10.47×10^{-4}, 13.96×10^{-4}, 17.45×10^{-4}, 20.94×10^{-4}, and 24.43×10^{-4} rad, respectively. The experimental results are shown in Fig. 3, which agree well with the theoretical expectation. The PCR in ω space denoted as R_ω shows a high sensitivity to a change of phase of the order of 10^{-4} rad. The black dotted line corresponds to Eq. (22), proving that R_ω is linearly proportional to v when the condition $|v| \ll \Delta\omega$ is satisfied.

In order to estimate the experimental uncertainty of the phase difference denoted as $\Delta\xi$, we may use the relation [42]

$$\Delta\xi = \frac{\Delta R_\omega}{\partial R_\omega/\partial\xi}. \tag{33}$$

Recording the postselected spectra at least 50 times with a time interval of one second, the standard deviation of the measured ΔR_ω with respect to ξ is presented in Fig. 4(a).

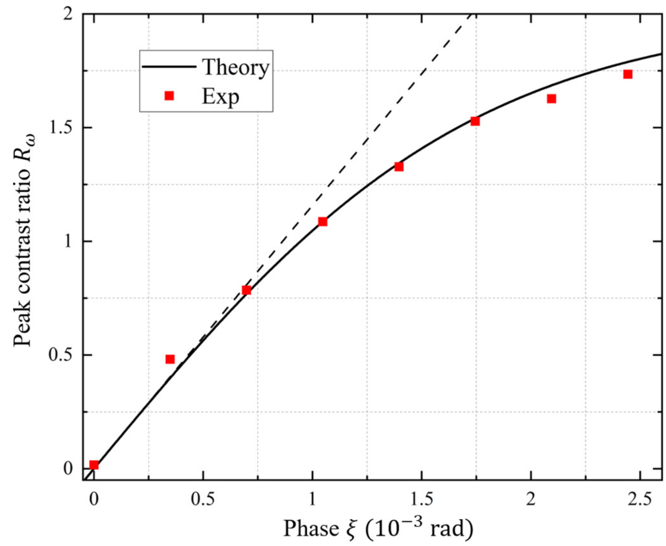

FIG. 3. The PCR R_ω in a function of the phase difference ξ. The red squares correspond to the experimental results and the black solid line corresponds to the theoretical prediction. The black dotted line shows the linear relation $R_\omega \simeq 2\sqrt{2}(\Delta\omega)^{-1}v$ when $|v| \ll \Delta\omega$.

The relation of ΔR_ω and ξ indicates that a greater intensity difference between the two peaks can make the output of the PCR pointer more stable. This property can be accounted for well by the noise analysis model established above. Since the sum $\Phi(x_3) + \Phi(x_1)$ detected increases with the increase of ξ, the fluctuations $R_\omega^\epsilon - R_\omega$ become smaller according to Eq. (26). By using Eq. (21), we then plot $\Delta\xi$ with respect to different ξ in Fig. 4(b). It can be seen that in spite of the fact that ΔR_ω reduces with the increase of ξ, the uncertainty $\Delta\xi$ eventually is proportional to ξ. We can lay the blame of increasing $\Delta\xi$ on the decreasing rate of $\partial R_\omega/\partial\xi$ being larger than the decreasing rate of ΔR_ω [see Eq. (33)]. It, finally, turns out that the experimental precision can be effectively retained at the order of 10^{-6} rad. Under exactly the same experimental conditions, this precision competes well with the precision 10^{-4} as (equivalent to a precision of phase of

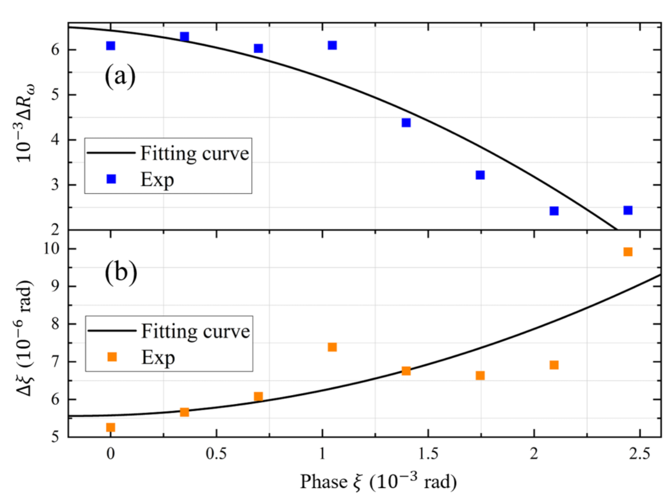

FIG. 4. (a) The experimental uncertainty of the PCR. (b) The experimental uncertainty of the phase difference.

10^{-6} rad) obtained in Ref. [16] where the SMV pointer was applied.

V. CONCLUSION

In conclusion, when the initial meter is Gaussian and the coupling strength is weak, the probability distribution after the postselection follows a bimodal function. We have shown that the PCR can be utilized as an alternative pointer to do weak measurement. We have found that in the linear response region, the PCR is linearly proportional to the quantity to be measured, while in the constant region, the PCR remains nearly unchanged. In practical applications, the working region should be kept away from the constant region. We have also demonstrated that the noise can be effectively suppressed. Furthermore, an experiment to measure a phase difference has been made. The experimental results agreed well with the theoretical expectation and the measured precision of the phase difference was retained at the order of 10^{-6} rad, which have confirmed the availability of the PCR pointer.

In order to further show the advantages of the PCR pointer, we will design a special measurement protocol in our future work. In the protocol, we place two multipixel photon counters, respectively, around where the two peaks locate and then correlate them with a lock-in amplifier. For the two photon counters, the detecting ranges can be narrow and the resolutions can be low, so that technically the dark current will be suppressed well and the response time will be greatly reduced. Therefore, we believe a weak measurement of higher efficiency and precision will be achieved when the PCR pointer is applied.

ACKNOWLEDGMENTS

This work is supported by the Natural Science Foundation of China (Grant No. 11674234), the Science Specialty Program of Sichuan University (Grant No.2020SCUNL210), and the Innovation Project of Sichuan University (Grant No. 2018SCUH0021).

APPENDIX A: WEAK MEASUREMENT APPROXIMATION

Without loss of generality, we may rewrite the condition given by Eq. (7) as

$$|\gamma(a_i - a_0)(p - p_0)| \ll 1, \tag{A1}$$

where a_0 is one of the eigenvalues a_i, and p_0 is one of the meter variables p.

When both a_0 and p_0 are equal to zero, it follows at once that $|\gamma a_i p| \ll 1$. So the exponential term in Eq. (5) can be expanded and held up to the first-order only, namely,

$$\exp(-i\gamma a_i \hat{p}) \simeq 1 - i\gamma a_i \hat{p}. \tag{A2}$$

Therefore, the weak measurement approximation presented in Eq. (7) can be considered reasonable. However, more generally, there exist some cases where none of a_i or p takes the value of zero. Under this circumstance, more detailed discussion is demanded.

In order to elucidate this question, we can express the operator corresponding to the measured quantity as

$$\hat{A} = \sum_i (a_i' + a_0)|a_i\rangle\langle a_i| = \sum_i a_i'|a_i\rangle\langle a_i| + a_0\hat{I}_A, \tag{A3}$$

where $a_i' = a_i - a_0$ and $\hat{I}_A$ denotes the system unit operator. Meanwhile, the operator corresponding to the meter variable can be written as

$$\hat{p} = \hat{p}' + p_0\hat{I}_p, \tag{A4}$$

where $\hat{I}_p$ denotes the meter unit operator. Now in a standard measurement, the coupled state of system and meter in x space is given by

$$\begin{aligned} |\psi_f(x)\rangle &= \langle x|\exp(-i\gamma\hat{A}\otimes\hat{p})|\psi\rangle|\psi_m\rangle \\ &= \langle x|\sum_i \exp[-i\gamma(a_i'\hat{p}' + a_0\hat{p}' + a_i'p_0 + a_0p_0)] \\ &\quad\times c_i|a_i\rangle|\psi_m\rangle, \end{aligned} \tag{A5}$$

where the unit operators are neglected for simplicity. It can be noted that the term $\exp(-i\gamma a_0\hat{p}')$ indicates a shift of γa_0 in x space of the meter wave function. For each eigenstate $|a_i\rangle$, the shifting value is the same, so that the term $\exp(-i\gamma a_0\hat{p}')$ is actually trivial and therefore can be suppressed. The terms $\sum_i \exp[-i\gamma(a_i'p_0 + a_0p_0)]$ indicate phases added to the system state, which can be suppressed by $\mathrm{U}_i(1)$ transformations, where the subscript i denotes each eigenstate $|a_i\rangle$. In addition, these $\mathrm{U}_i(1)$ transformations can be realized by an appropriate choice of the preselection. Therefore eventually Eq. (A5) can be simplified to

$$|\psi_f(x)\rangle = \langle x|\sum_i \exp(-i\gamma a_i'\hat{p}')c_i|a_i\rangle|\psi_m\rangle. \tag{A6}$$

According to the condition given by Eq. (A1), the weak measurement approximation in Eq. (8) is generally tenable.

APPENDIX B: CALCULATION OF THE DISTRIBUTION FUNCTIONS

The distribution function after postselection in x space is given by

$$\begin{aligned} \Phi(x) &= \mathrm{Tr}[(|x\rangle\langle x|\otimes\Pi_\phi)U(\rho\otimes\rho_m)U^\dagger] \\ &= \langle x|\langle\phi|U|\psi\rangle|\psi_m\rangle\langle\psi_m|\langle\psi|U^\dagger|\phi\rangle|x\rangle \\ &\simeq |\langle x|\langle\phi|(1 - i\gamma\hat{A}\otimes\hat{p})|\psi\rangle|\psi_m\rangle|^2 \\ &= |\langle\phi|\psi\rangle\left[\psi_m(x) - \gamma A_w\frac{\partial}{\partial x}\psi_m(x)\right]|^2 \\ &\propto \left\{1 + \frac{\gamma(x-\bar{x})}{(\Delta x)^2}\mathrm{Re}A_w + \left[\frac{\gamma(x-\bar{x})}{2(\Delta x)^2}\right]^2|A_w|^2\right\} \\ &\quad\times|\langle\phi|\psi\rangle|^2\exp\left[-\frac{(x-\bar{x})^2}{2(\Delta x)^2}\right], \end{aligned} \tag{B1}$$

in the fourth line of which the relation $\hat{p}|x\rangle = i\frac{\partial}{\partial x}|x\rangle$ is used. So using the other relation $\hat{p}|p\rangle = p|p\rangle$ and following the same procedure as presented, the distribution function after postselection in p space can be obtained immediately.

APPENDIX C: DERIVATION OF THE SMV WHEN THE NOISE IS INTRODUCED

When the noise is taken into account, the SMV is given by

$$\begin{aligned}\delta\langle x\rangle^{\epsilon} &= \frac{\int_{-\infty}^{+\infty}(x-\bar{x})[\Phi(x)+\epsilon(x)]dx}{\int_{-\infty}^{+\infty}[\Phi(x)+\epsilon(x)]dx}\\ &= \frac{\int_{-\infty}^{+\infty}(x-\bar{x})[\Phi(x)+\frac{a}{1+b}]dx}{\int_{-\infty}^{+\infty}[\Phi(x)+\frac{a}{1+b}]dx}.\end{aligned} \tag{C1}$$

Since $\frac{a}{1+b}$ is not integrable on $(-\infty,+\infty)$ and, in practice, the detecting range of the apparatus is always confined, we change the integrating range to $[\bar{x}-r,\bar{x}+r]$ and let $2r$ be large enough to make $\int_{-\infty}^{+\infty}\Phi(x)dx \simeq \int_{\bar{x}-r}^{\bar{x}+r}\Phi(x)dx$. On the other hand, we also assume that the integrating range is not too broad so that we will have $\int_{\bar{x}-r}^{\bar{x}+r}\Phi(x)dx \gg \int_{\bar{x}-r}^{\bar{x}+r}adx$. Then the SMV can be further written as

$$\begin{aligned}\delta\langle x\rangle^{\epsilon} &= \frac{\int_{\bar{x}-r}^{\bar{x}+r}(x-\bar{x})\Phi(x)dx}{\int_{\bar{x}-r}^{\bar{x}+r}\Phi(x)dx+\int_{\bar{x}-r}^{\bar{x}+r}\frac{a}{1+b}dx}\\ &\simeq \frac{\int_{\bar{x}-r}^{\bar{x}+r}(x-\bar{x})\Phi(x)dx}{\int_{\bar{x}-r}^{\bar{x}+r}\Phi(x)dx+\int_{\bar{x}-r}^{\bar{x}+r}a(1-b)dx}\\ &\simeq \delta\langle x\rangle\left[1-\frac{2ar}{\int_{\bar{x}-r}^{\bar{x}+r}\Phi(x)dx}\right],\end{aligned} \tag{C2}$$

where all the higher-order terms are neglected. Applying the mean value theorem, it follows at once that $\int_{\bar{x}-r}^{\bar{x}+r}\Phi(x)dx = 2r\Phi(x_0)$, where $x_0 \in [\bar{x}-r,\bar{x}+r]$. Hence, finally, we obtain

$$\delta\langle x\rangle^{\epsilon} \simeq \delta\langle x\rangle\left[1-\frac{a}{\Phi(x_0)}\right]. \tag{C3}$$

Considering the so-called three-sigma rule for the Gaussian function, $\Phi(x_0)$ may be determined by the simple relation

$$\begin{aligned}\Phi(x_0) &\simeq \frac{1}{6\Delta x}\int_{-\infty}^{+\infty}\Phi(x)dx\\ &= \frac{1}{6\Delta x}\left[1+\left(\frac{\gamma}{2\Delta x}\right)^2|A_w|^2\right]|\langle\phi|\psi\rangle|^2.\end{aligned} \tag{C4}$$

APPENDIX D: POSTSELECTION APPLIED IN THE EXPERIMENT

The combination of a quarter wave plate and a polarizer has been successfully applied as the postselection in Ref. [43] when the incident light is monochromatic. Here we will demonstrate that this kind of postselection also works for the case where the incident light is polychromatic but the bandwidth of which is narrow.

On the basis of the horizontal and vertical polarization states $|H\rangle$ and $|V\rangle$, the function of a quarter wave plate (QWP) whose optical axis is set at -45° can be illustrated in the matrix form

$$\text{QWP} = \begin{pmatrix}\cos\tau_0\omega & -i\sin\tau_0\omega\\ -i\sin\tau_0\omega & \cos\tau_0\omega\end{pmatrix}, \tag{D1}$$

where τ_0 denotes a time delay determined by the thickness of the QWP. When the incident light is monochromatic and the angular frequency ω_c of which matches the QWP, it turns out that $\tau_0\omega_c = \pi/4$. However, for the case of polychromatic incident light, we may rewrite $\gamma_0\omega$ as the following form:

$$\begin{aligned}\tau_0\omega &= \tau_0(\omega_c+\delta\omega)\\ &= \tau_0\omega_c(1+\delta\omega/\omega_c).\end{aligned} \tag{D2}$$

Now if the bandwidth is narrow so that the relation $\delta\omega/\omega_c \ll 1$ is satisfied, then we may have $\tau_0\omega \simeq \tau_0\omega_c$. Under this circumstance, the matrix above reads

$$\text{QWP} \simeq \frac{1}{\sqrt{2}}\begin{pmatrix}1 & -i\\ -i & 1\end{pmatrix}. \tag{D3}$$

Therefore, the postselection takes the following form:

$$\begin{aligned}|\phi\rangle &\simeq \frac{1}{\sqrt{2}}\begin{pmatrix}1 & -i\\ -i & 1\end{pmatrix}\begin{pmatrix}\cos(\varphi-\pi/4)\\ \sin(\varphi-\pi/4)\end{pmatrix}\\ &= \frac{1}{\sqrt{2}}\exp(i\pi/4)\begin{pmatrix}\exp(-i\varphi)\\ -\exp(i\varphi)\end{pmatrix}\\ &= \frac{1}{\sqrt{2}}[\exp(-i\varphi)|H\rangle-\exp(i\varphi)|V\rangle],\end{aligned} \tag{D4}$$

where the phase term $\exp(-i\pi/4)$ in the third line is neglected since it makes no difference to the distribution functions.

[1] J. Von Neumann, *Mathematical Foundations of Quantum Mechanics: New Edition* (Princeton University Press, Princeton, NJ, 2018).

[2] Y. Aharonov, P. G. Bergmann, and J. L. Lebowitz, Phys. Rev. **134**, B1410 (1964).

[3] Y. Aharonov, D. Z. Albert, and L. Vaidman, Phys. Rev. Lett. **60**, 1351 (1988).

[4] N. W. M. Ritchie, J. G. Story, and R. G. Hulet, Phys. Rev. Lett. **66**, 1107 (1991).

[5] O. Hosten and P. Kwiat, Science **319**, 787 (2008).

[6] W. Long, J. Pan, X. Guo, X. Liu, H. Lin, H. Zheng, J. Yu, H. Guan, H. Lu, Y. Zhong, S. Fu, L. Zhang, W. Zhu, and Z. Chen, Photon. Res. **7**, 1273 (2019).

[7] R. Wang, J. Zhou, K. Zeng, S. Chen, X. Ling, W. Shu, H. Luo, and S. Wen, APL Photon. **5**, 016105 (2020).

[8] B. Xia, J. Huang, C. Fang, H. Li, and G. Zeng, Phys. Rev. Appl. **13**, 034023 (2020).

[9] P. B. Dixon, D. J. Starling, A. N. Jordan, and J. C. Howell, Phys. Rev. Lett. **102**, 173601 (2009).

[10] S. Kocsis, B. Braverman, S. Ravets, M. J. Stevens, R. P. Mirin, L. K. Shalm, and A. M. Steinberg, Science **332**, 1170 (2011).

[11] W. Wu, S. Chen, W. Xu, Z. Liu, R. Lou, L. Shen, H. Luo, S. Wen, and X. Yin, Photon. Res. B **8**, B47 (2020).

[12] N. Brunner and C. Simon, Phys. Rev. Lett. **105**, 010405 (2010).

[13] X.-Y. Xu, Y. Kedem, K. Sun, L. Vaidman, C.-F. Li, and G.-C. Guo, Phys. Rev. Lett. **111**, 033604 (2013).

[14] L. J. Salazar-Serrano, D. Janner, N. Brunner, V. Pruneri, and J. P. Torres, Phys. Rev. A **89**, 012126 (2014).

[15] C. Fang, J.-Z. Huang, Y. Yu, Q. Li, and G. Zeng, J. Phys. B: At., Mol. Opt. Phys. **49**, 175501 (2016).

[16] Z. Li, L. Xie, Q. Ti, P. Duan, Z. Zhang, and C. Ren, Phys. Rev. A **102**, 023701 (2020).
[17] Y. Xu, L. Shi, T. Guan, S. Zhong, X. Zhou, D. Li, C. Guo, Y. Yang, X. Wang, Z. Li, Y. He, L. Xie, and Z. Gan, Appl. Phys. Lett. **114**, 181901 (2019).
[18] D. Li, T. Guan, F. Liu, A. Yang, Y. He, Q. He, Z. Shen, and M. Xin, Appl. Phys. Lett. **112**, 213701 (2018).
[19] Y. Yang, Y. Xu, T. Guan, L. Shi, J. Li, D. Li, Y. He, X. Wang, Z. Li, and Y. Ji, IEEE Photon. J. **12**, 1 (2020).
[20] I. Shomroni, O. Bechler, S. Rosenblum, and B. Dayan, Phys. Rev. Lett. **111**, 023604 (2013).
[21] G. I. Viza, J. Martínez-Rincón, G. A. Howland, H. Frostig, I. Shomroni, B. Dayan, and J. C. Howell, Opt. Lett. **38**, 2949 (2013).
[22] O. S. Magaña Loaiza, M. Mirhosseini, B. Rodenburg, and R. W. Boyd, Phys. Rev. Lett. **112**, 200401 (2014).
[23] G. Chen, N. Aharon, Y.-N. Sun, Z.-H. Zhang, W.-H. Zhang, D.-Y. He, J.-S. Tang, X.-Y. Xu, Y. Kedem, C.-F. Li *et al.*, Nat. Commun. **9**, 93 (2018).
[24] G. Chen, L. Zhang, W.-H. Zhang, X.-X. Peng, L. Xu, Z.-D. Liu, X.-Y. Xu, J.-S. Tang, Y.-N. Sun, D.-Y. He, J.-S. Xu, Z.-Q. Zhou, C.-F. Li, and G.-C. Guo, Phys. Rev. Lett. **121**, 060506 (2018).
[25] A. G. Kofman, S. Ashhab, and F. Nori, Phys. Rep. **520**, 43 (2012).
[26] C. Ferrie and J. Combes, Phys. Rev. Lett. **112**, 040406 (2014).
[27] G. C. Knee and E. M. Gauger, Phys. Rev. X **4**, 011032 (2014).
[28] D. J. Starling, P. B. Dixon, A. N. Jordan, and J. C. Howell, Phys. Rev. A **80**, 041803(R) (2009).
[29] A. N. Jordan, J. Martínez-Rincón, and J. C. Howell, Phys. Rev. X **4**, 011031 (2014).
[30] J. Sinclair, M. Hallaji, A. M. Steinberg, J. Tollaksen, and A. N. Jordan, Phys. Rev. A **96**, 052128 (2017).
[31] K. Lyons, J. Dressel, A. N. Jordan, J. C. Howell, and P. G. Kwiat, Phys. Rev. Lett. **114**, 170801 (2015).
[32] D. J. Starling, P. B. Dixon, N. S. Williams, A. N. Jordan, and J. C. Howell, Phys. Rev. A **82**, 011802(R) (2010).
[33] G. C. Knee and W. J. Munro, Phys. Rev. A **92**, 012130 (2015).
[34] J. M. Hogan, J. Hammer, S.-W. Chiow, S. Dickerson, D. M. S. Johnson, T. Kovachy, A. Sugarbaker, and M. A. Kasevich, Opt. Lett. **36**, 1698 (2011).
[35] C. Gerry, P. Knight, and P. L. Knight, *Introductory Quantum Optics* (Cambridge University Press, Cambridge, 2005).
[36] J. Dressel, M. Malik, F. M. Miatto, A. N. Jordan, and R. W. Boyd, Rev. Mod. Phys. **86**, 307 (2014).
[37] R. Jozsa, Phys. Rev. A **76**, 044103 (2007).
[38] J. Dressel and A. N. Jordan, Phys. Rev. A **85**, 012107 (2012).
[39] K. Ogawa, H. Kobayashi, and A. Tomita, Phys. Rev. A **101**, 042117 (2020).
[40] K. Ogawa, O. Yasuhiko, H. Kobayashi, T. Nakanishi, and A. Tomita, New J. Phys. **21**, 043013 (2019).
[41] A. J. Jerri, Proc. IEEE **65**, 1565 (1977).
[42] S. Pang and T. A. Brun, Phys. Rev. Lett. **115**, 120401 (2015).
[43] X. Qiu, L. Xie, X. Liu, L. Luo, Z. Li, Z. Zhang, and J. Du, Appl. Phys. Lett. **110**, 071105 (2017).